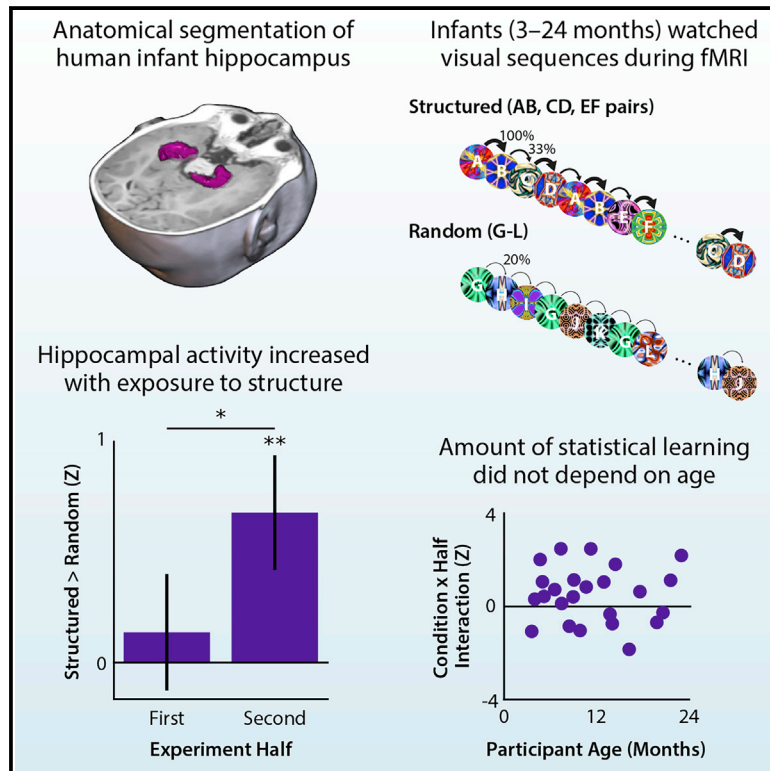


## Evidence of hippocampal learning in human infants

## Graphical abstract



## Authors

Cameron T. Ellis, Lena J. Skalaban,  
Tristan S. Yates, Vikranth R. Bejjanki,  
Natalia I. Córdoba,  
Nicholas B. Turk-Browne

## Correspondence

nicholas.turk-browne@yale.edu

## In brief

Ellis et al. use fMRI to study how human infants learn from experience. Despite substantial anatomical changes over the first 2 years of life, the hippocampus supports statistical learning from early infancy. This establishes how the infant brain is prepared for rapid and prodigious learning throughout development.

## Highlights

- Hippocampus supports statistical learning of temporal regularities in infancy
- Changes in hippocampal activity emerge after only minutes of exposure
- Localization of learning effects within hippocampal system similar to adults
- Exploratory analyses suggest a selective role for medial prefrontal cortex



## Report

## Evidence of hippocampal learning in human infants

Cameron T. Ellis,<sup>1</sup> Lena J. Skalaban,<sup>1</sup> Tristan S. Yates,<sup>1</sup> Vikranth R. Bejjanki,<sup>2</sup> Natalia I. Córdoba,<sup>1</sup> and Nicholas B. Turk-Browne<sup>1,3,\*</sup>

<sup>1</sup>Department of Psychology, Yale University, 2 Hillhouse Avenue, New Haven, CT 06511, USA

<sup>2</sup>Department of Psychology, Hamilton College, 198 College Hill Road, Clinton, NY 13323, USA

<sup>3</sup>Lead contact

\*Correspondence: [nicholas.turk-browne@yale.edu](mailto:nicholas.turk-browne@yale.edu)

<https://doi.org/10.1016/j.cub.2021.04.072>

## SUMMARY

The hippocampus is essential for human memory.<sup>1</sup> The protracted maturation of memory capacities from infancy through early childhood<sup>2–4</sup> is thus often attributed to hippocampal immaturity.<sup>5–7</sup> The hippocampus of human infants has been characterized in terms of anatomy,<sup>8,9</sup> but its function has never been tested directly because of technical challenges.<sup>10,11</sup> Here, we use recently developed methods for task-based fMRI in awake human infants<sup>12</sup> to test the hypothesis that the infant hippocampus supports statistical learning.<sup>13–15</sup> Hippocampal activity increased with exposure to visual sequences of objects when the temporal order contained regularities to be learned, compared to when the order was random. Despite the hippocampus doubling in anatomical volume across infancy, learning-related functional activity bore no relationship to age. This suggests that the hippocampus is recruited for statistical learning at the youngest ages in our sample, around 3 months. Within the hippocampus, statistical learning was clearer in anterior than posterior divisions. This is consistent with the theory that statistical learning occurs in the monosynaptic pathway,<sup>16</sup> which is more strongly represented in the anterior hippocampus.<sup>17,18</sup> The monosynaptic pathway develops earlier than the trisynaptic pathway, which is linked to episodic memory,<sup>19,20</sup> raising the possibility that the infant hippocampus participates in statistical learning before it forms durable memories. Beyond the hippocampus, the medial prefrontal cortex showed statistical learning, consistent with its role in adult memory integration<sup>21</sup> and generalization.<sup>22</sup> These results suggest that the hippocampus supports the vital ability of infants to extract the structure of their environment through experience.

## RESULTS

## Role of infant hippocampus in statistical learning

We collected brain imaging data across 24 sessions (lab visits) from 17 unique infants (14 sessions from 10 females) aged 3–24 months. We defined anatomical regions of interest (ROIs) using a structural MRI obtained in each session (Figure 1A). We manually segmented the hippocampus bilaterally from the surrounding medial temporal lobe (MTL) cortex. The volume of the hippocampal ROIs was strongly related to age (left  $b = 68.0 \text{ mm}^3/\text{month}$ ,  $r = 0.88$ ,  $p < 0.001$ ; right  $b = 68.5 \text{ mm}^3/\text{month}$ ,  $r = 0.84$ ,  $p < 0.001$ ), with the hippocampus approximately doubling in volume over the age range (Figure 1B). Global brain volume increased dramatically with age too ( $r = 0.90$ ;  $p < 0.001$ ), but the change in bilateral hippocampal volume persisted after controlling for this global growth ( $r_{\text{partial}} = 0.44$ ;  $p = 0.005$ ). This suggests that the hippocampus grows rapidly in size during infancy, at a faster rate than average in the brain.

We used fMRI to measure activity in the hippocampus during a statistical learning task. Infants viewed continuous sequences of colorful, fractal-like objects that appeared dynamically in a looming motion. The sequences were presented in blocks that alternated between structured and random conditions.<sup>14</sup> In structured blocks (Figure 2A), temporal regularities were embedded in the sequence: fractals appeared in pairs such that the first

fractal was always followed by the second. In random blocks (Figure 2B), there were no regularities in the sequence: all fractals were equally likely to follow each other. Different sets of fractals were used for structured and random blocks (counterbalanced across sessions), but the fractal set for a given condition was held constant across blocks, as were the pairs generated from the structured set. Other than the lack of regularities, the random condition was closely matched to the structured condition, including the number, frequency, and timing of fractals. Any difference in brain activity between structured and random blocks can thus be attributed to the regularities in structured blocks.<sup>23</sup> Importantly, representing these regularities required learning: pairs could only be extracted from the continuous sequence by encoding and integrating repeating patterns of co-occurrence. In other words, because pairings were arbitrary, at any given moment in a structured block, it was impossible to know which fractals were paired; the pairs only existed in the mind of the observer because of the history of how the fractals appeared together earlier in the block or in preceding blocks.

To capture this learning over time, we divided the blocks in each condition into the first half of exposure (when we expected less evidence of learning) and the second half of exposure (when we expected more robust learning effects). We then calculated the difference in blood-oxygen-level-dependent (BOLD) response in the bilateral hippocampus between structured and

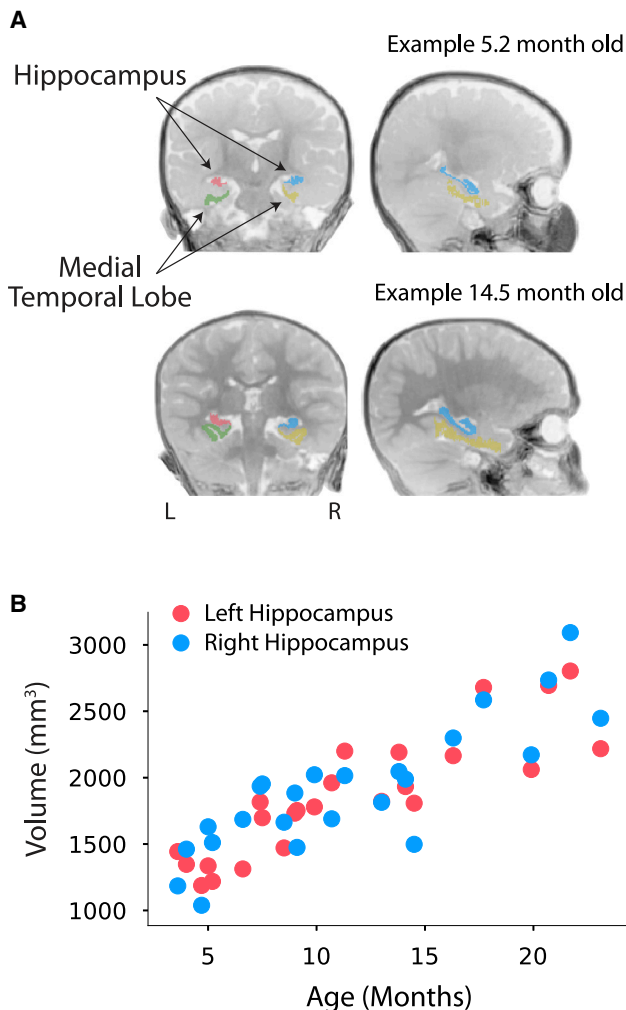


**Figure 1. Hippocampal regions of interest**

(A) Anatomical segmentation of the infant hippocampus and medial temporal lobe cortex in two representative participants, aged 5.2 (top) and 14.5 (bottom) months. Intensity of brain images inverted to highlight gray matter.

(B) Volume of the left and right hippocampus by participant age. Each session is represented by a red and blue dot at the same age coordinate.

See also Figure S3.

random blocks (Figure 3A). In the first half, there was no difference in hippocampal activity between structured and random blocks ( $M = 0.14$ ; confidence interval [CI] =  $[-0.358, 0.656]$ ;  $p = 0.614$ ). However, in the second half, there was significantly greater hippocampal activity in structured than random blocks ( $M = 0.67$ ; CI =  $[0.172, 1.176]$ ;  $p = 0.007$ ). This difference in the second half was larger than in the first half, as revealed by significant interaction between condition and half ( $M = 0.50$ ; CI =  $[0.028, 0.966]$ ;  $p = 0.037$ ). This learning-related interaction did not differ based on whether infants encountered a structured or random block first ( $M = -0.51$ ; CI =  $[-1.503, 0.454]$ ;  $p = 0.296$ ). Although infants looked less in the second than first half ( $M = -0.10$ ; CI =  $[-0.187, -0.015]$ ;  $p = 0.021$ ), perhaps reflecting boredom or fatigue, there were no differences in looking time between structured and random blocks ( $M = 0.06$ ; CI =  $[-0.013, 0.146]$ ;  $p = 0.107$ ), nor was there an interaction in

gaze behavior between condition and half ( $M = 0.02$ ; CI =  $[-0.057, 0.104]$ ;  $p = 0.604$ ).

The hippocampal interaction between condition and half did not significantly correlate with infant age (Figure 3B;  $r = -0.03$ ;  $p = 0.893$ ). Bayesian regression<sup>24</sup> found what is considered “anecdotal” evidence<sup>25</sup> in favor of the null hypothesis of no age relationship (Bayes factor = 0.376). This null did not reflect a general inability to resolve age relationships in our sample, as hippocampal volume reliably increased (Figure 1B). Hippocampal volume did not relate to the interaction effect ( $r = -0.05$ ;  $p = 0.775$ ) and, when controlling for hippocampal volume, the relationship between the interaction effect and age remained non-significant ( $r = 0.03$ ;  $p = 0.883$ ). These findings suggest that, from as young as 3 months old, the hippocampus is able to support statistical learning. This represents the first evidence of task-related activity in the hippocampus of human infants to our knowledge.

### Subdivisions of the hippocampus

We hypothesized that the hippocampus is involved in infant statistical learning partly because of the early development of the monosynaptic pathway from entorhinal cortex to CA1.<sup>16,19,20</sup> There are no established protocols for segmenting hippocampal subfields in infants that would allow us to directly assay CA1, and so instead we used the longitudinal axis of the hippocampus as a proxy (Figure 3C). Namely, the anterior hippocampus contains more of CA1 than posterior hippocampus,<sup>17,18</sup> and so we predicted clearer evidence of statistical learning in the anterior hippocampus (Figure 3E). Indeed, whereas the anterior hippocampus showed no difference between structured and random blocks in the first half ( $M = 0.07$ ; CI =  $[-0.489, 0.648]$ ;  $p = 0.846$ ), there was a robust difference in the second half ( $M = 0.73$ ; CI =  $[0.202, 1.257]$ ;  $p = 0.006$ ) and a significant interaction between condition and half ( $M = 0.58$ ; CI =  $[0.091, 1.063]$ ;  $p = 0.018$ ). The posterior hippocampus again showed no difference in the first half ( $M = 0.23$ ; CI =  $[-0.216, 0.727]$ ;  $p = 0.328$ ), but the difference in the second half was numerically weaker than in the anterior hippocampus ( $M = 0.60$ ; CI =  $[0.062, 1.112]$ ;  $p = 0.028$ ) and the interaction did not reach significance ( $M = 0.39$ ; CI =  $[-0.106, 0.879]$ ;  $p = 0.119$ ); the interaction in posterior was not significantly weaker than in anterior ( $M = 0.19$ ; CI =  $[-0.086, 0.477]$ ;  $p = 0.174$ ).

We also divided the hippocampus into left and right hemispheres. Adult fMRI studies have reported statistical learning effects more consistently in the right hippocampus.<sup>23,26</sup> This same pattern was found in infants (Figure 3D), with clearer evidence of statistical learning in the right hippocampus (first half:  $M = 0.09$ , CI =  $[-0.428, 0.635]$ ,  $p = 0.759$ ; second half:  $M = 0.75$ , CI =  $[0.243, 1.243]$ ,  $p = 0.003$ ; interaction:  $M = 0.60$ , CI =  $[0.116, 1.090]$ ,  $p = 0.013$ ) than in the left hippocampus (first half:  $M = 0.20$ , CI =  $[-0.345, 0.754]$ ,  $p = 0.500$ ; second half:  $M = 0.59$ , CI =  $[0.021, 1.132]$ ,  $p = 0.043$ ; interaction:  $M = 0.38$ , CI =  $[-0.135, 0.890]$ ,  $p = 0.155$ ); the interaction in left was not significantly weaker than in right ( $M = 0.22$ ; CI =  $[-0.106, 0.574]$ ;  $p = 0.207$ ). Above, we treated comparisons between anterior and posterior and left and right hippocampus separately based on distinct theoretical motivations. However, we found evidence that these divisions interact ( $M = -0.52$ ; CI =  $[-0.903, -0.164]$ ;  $p = 0.003$ ). Namely, a hemispheric difference in the learning

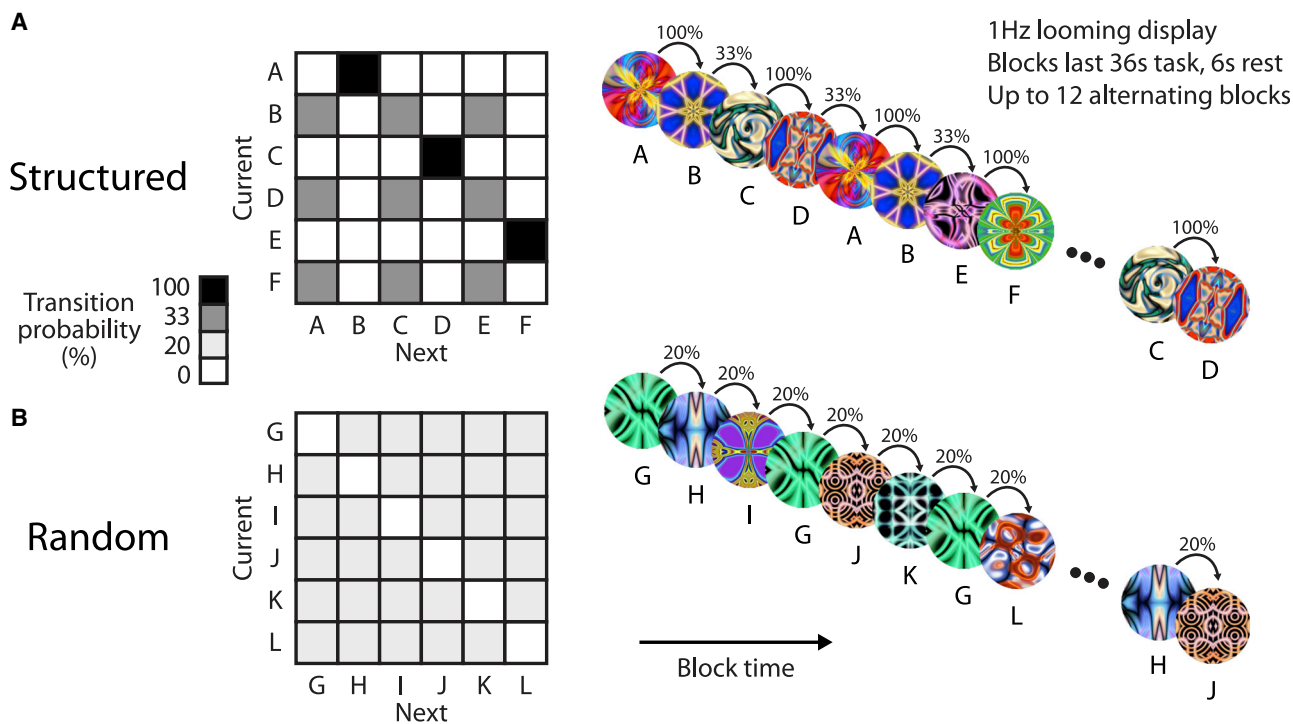


**Figure 2. Statistical learning task design**

Participants viewed colorful fractals one at a time in blocks. The blocks alternated between structured and random conditions within participant. Different fractals were shown in each condition but remained consistent over blocks.

(A) In structured blocks, fractals were grouped into three pairs (AB, CD, EF), with the first member of a pair (e.g., A) always followed by the second (e.g., B), which in turn was followed by the beginning of the next pair without interruption. As a result, the pairs could only be learned based on the transition probabilities in the sequence (100% within pair; 33% between pairs).

(B) In random blocks, fractals (G, H, I, J, K, and L) appeared in a random order with no back-to-back repetitions. As a result, there was no structure in their transition probabilities (uniform 20%). Because fractals were randomly assigned to the conditions and individually appeared an equal number of times within and across blocks (to equate familiarity), the conditions differed only in the opportunity for statistical learning. Participants completed up to 12 blocks, and usable blocks were split into the first and second half of exposure.

See also [Table S1](#).

effect was more apparent in posterior than anterior hippocampus ([Figure S1](#)). In sum, the overall pattern of learning-related signals across the longitudinal and hemispheric axes of the infant hippocampus is consistent with primate anatomy,<sup>19,20</sup> computational models,<sup>16</sup> and adult function.<sup>23,26</sup>

### Time course of hippocampal involvement

Splitting the fMRI data into the first and second half of exposure in the main analyses was an attempt to capture learning over time while retaining enough blocks per time bin to estimate stable effects. We also examined learning over time more continuously at the block level ([Figure S2](#)). Adopting a supersubject approach, we pooled usable blocks across sessions and assessed statistical significance with bootstrap resampling. The difference between structured and random blocks was largest and only statistically significant in the fifth and sixth blocks (of six). In other words, neural evidence of statistical learning emerged after about 2 min of exposure to structured blocks (four blocks of 36 s). This amount of exposure is consistent with the duration of classic behavioral studies of statistical learning in infants.<sup>14,15</sup> This suggests that fMRI can serve as a sensitive, converging measure of infant cognition, even for relatively short task designs.

### Engagement of neocortical systems

Although the hippocampus was the focus of this study, we also compared structured and random blocks in surrounding MTL cortex. Despite being anatomically adjacent and a larger ROI, we found only weak evidence of statistical learning in MTL cortex ([Figure S3](#)), highlighting the selectivity of our results to the hippocampus within the broader MTL. We additionally performed exploratory voxelwise analyses across the whole brain with data aligned to standard space ([Figure 4](#)). The key learning interaction in the hippocampus between condition (structured versus random) and half (second versus first) was found elsewhere only in medial prefrontal cortex (mPFC) after correction for multiple comparisons ( $t_{(23)} = 5.13$ ; corrected  $p = 0.048$ ; 116 voxels; MNI:  $-5, 53, 4$ ). Involvement of mPFC in statistical learning is consistent with its role in memory integration<sup>21</sup> and generalization.<sup>22</sup> The mPFC and hippocampus are both part of the default mode network.<sup>27</sup> Thus, an alternative explanation for their greater activity in the second half of the structured condition could be an increase in task disengagement (e.g., habituation, boredom, self-reflection). Inconsistent with this possibility, a follow-up analysis of other default mode regions did not exhibit the same interaction ([Figure S4](#)).

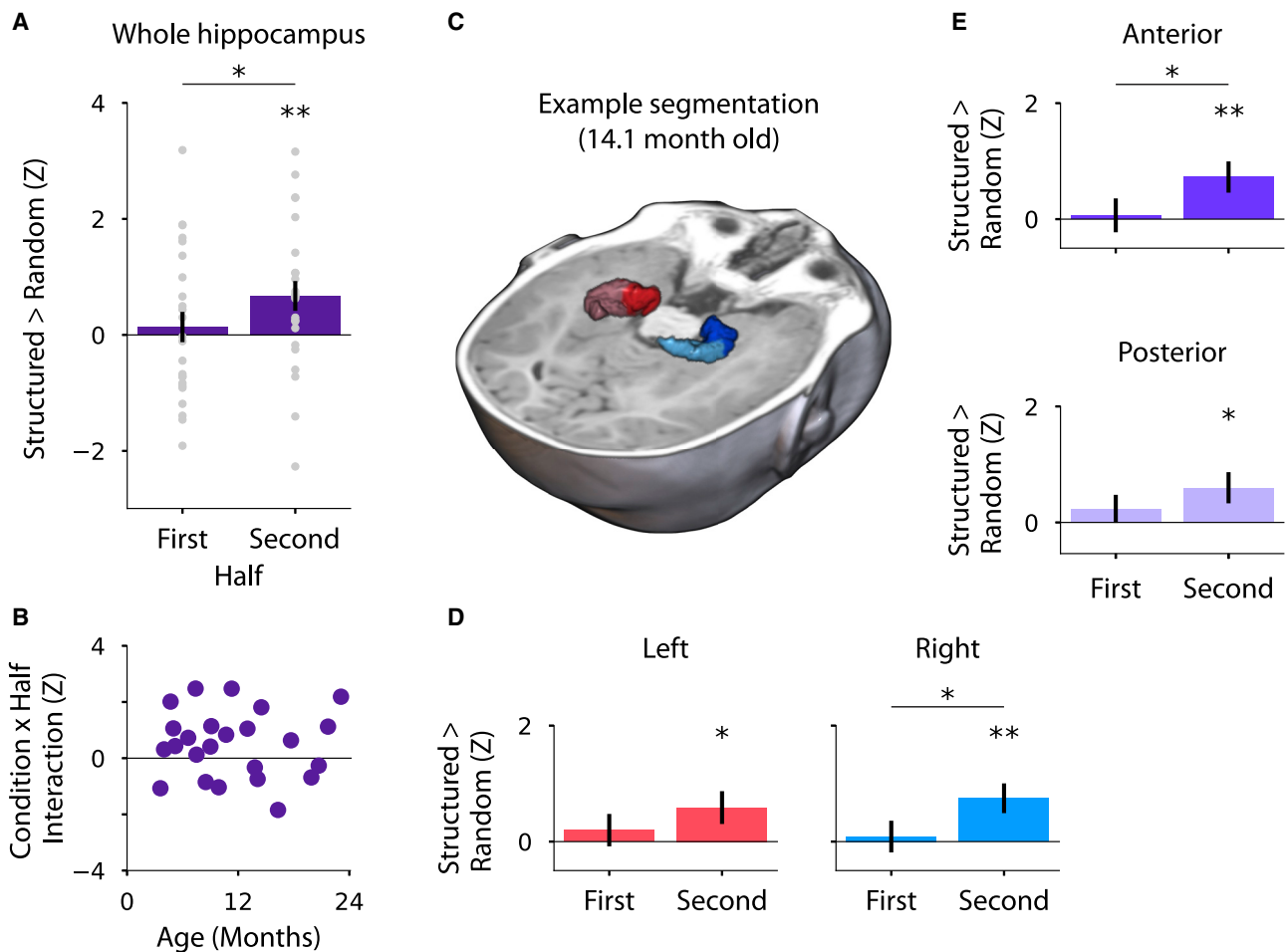


**Figure 3. Neural evidence of statistical learning in infant hippocampus**

(A) Mean difference in normalized parameter estimates of BOLD activity between structured and random blocks in bilateral hippocampus. A reliable difference emerged by the second half, which was significantly greater than in the first half. Each gray dot is one session.

(B) Using the interaction between condition and half as a metric of hippocampal statistical learning, there was no relationship with participant age.

(C) Three-dimensional rendering of an example hippocampal segmentation (14.1 months old).

(D and E) Mean difference in BOLD activity between structured and random blocks in (D) left (red) and right (blue) hippocampus and in (E) anterior (dark) and posterior (light) hippocampus.

Error bars reflect standard error of the mean across sessions within half. \* $p < 0.05$ ; \*\* $p < 0.01$ . See also [Figures S1](#) and [S2](#).

## DISCUSSION

We present the first study that uses fMRI to study cognitive, rather than visual or auditory,<sup>28–30</sup> processing in infants. The key finding of this study is that activity in the hippocampus of human infants increases through exposure to regularities. This activity may correspond to different stages of statistical learning. It could reflect the process of extracting regularities during learning, with differences emerging in the second half because a certain amount of exposure was needed to compute the transition probabilities between fractals and represent the pairs. In adults, the hippocampus is often recruited more strongly early in learning,<sup>31,32</sup> when stimuli are novel.<sup>33</sup> Hence, it is possible that greater hippocampal activity for structured versus random in the second half would eventually dissipate or reverse if we continued to present blocks. How much exposure results in increased versus decreased hippocampal

activity with learning will likely depend on the complexity of information to be learned (e.g., discrete items versus statistical relationships) and on the nature of the task (e.g., incidental versus intentional encoding).

It is also possible that greater hippocampal activity for structured versus random would persist with more exposure, if this activity reflects additional cognitive processes triggered by the regularities. In particular, the first item of each learned pair in structured blocks may trigger a hippocampal process of prediction or pattern completion of the second item.<sup>34,35</sup> In addition to clarifying the timing and consequences of hippocampal participation in infant statistical learning, future research is needed to determine whether this role is necessary for behavioral expression of statistical learning. This will be difficult to test in infants, but studies in adult patients with hippocampal damage suggest that the hippocampus may in fact be necessary for normal statistical learning behavior.<sup>36,37</sup>



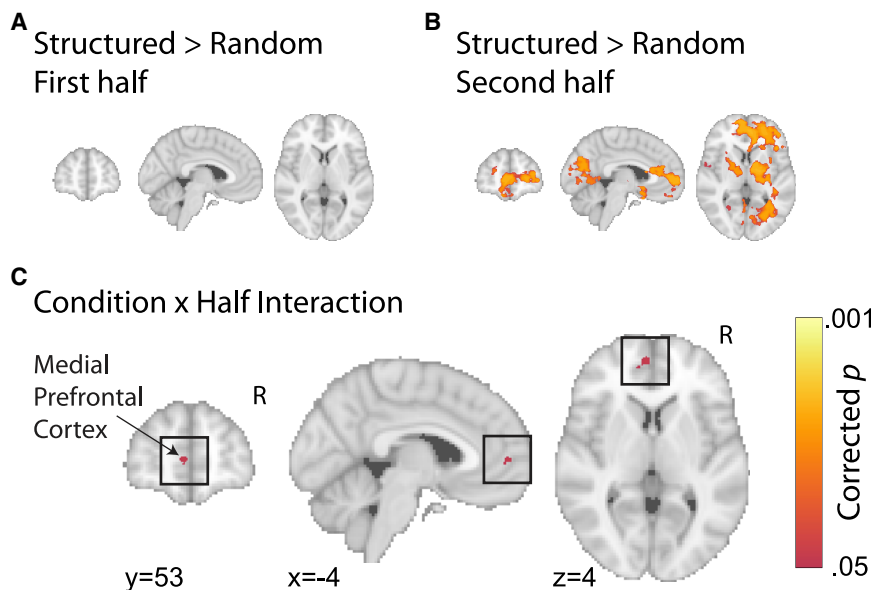


**Figure 4. Exploratory whole-brain analysis** (A and B) Voxelwise contrast of BOLD activity between structured and random blocks in (A) the first half and (B) the second half. (C) The medial prefrontal cortex (mPFC) showed an interaction between condition and half, with a greater difference between structured and random in the second versus first half. Voxels in color were significant after correction for multiple comparisons (threshold-free cluster enhancement; one-tailed corrected  $p < 0.05$ ). Coordinates are in MNI space. See also Figure S4.

The involvement of the infant hippocampus in statistical learning has implications for theories of memory. According to complementary learning systems,<sup>38</sup> episodic memory is a precursor to statistical learning. The hippocampus rapidly encodes individual experiences and then, through a process of consolidation, the neocortex gradually generalizes across these episodic memories to extract regularities. Infants present a conundrum for this framework: they show robust statistical learning,<sup>14,15</sup> despite impoverished episodic memory.<sup>2–4</sup> A recent update to the theory<sup>16</sup> suggests a potential resolution, at least for the rapid form of statistical learning in our study. Neural network simulations showed that such statistical learning can occur within the hippocampus itself in a way that bypasses the circuitry for episodic memory. Thus, the hippocampus may support statistical learning in infants, as reported in this study, before it can support episodic memory. We show that the hippocampus grows substantially in size during infancy<sup>9</sup> yet find that evidence of statistical learning in hippocampal activity does not increase over the same period. Speculatively, anatomical growth of the hippocampus over infancy may support the emergence of episodic memory. This would be consistent with the slower development in primate hippocampus<sup>20</sup> of the trisynaptic pathway, linked to episodic memory, than the monosynaptic pathway, linked to statistical learning.<sup>16</sup> Indeed, this pattern continues through childhood, with a shift in relative volume from anterior to posterior hippocampus that correlates with episodic memory.<sup>39,40</sup> Alternatively, episodic memory may be more developed in infants than currently known—consistent with recent rodent work<sup>41,42</sup>—such that the hippocampal statistical learning we report may in fact be dependent upon episodic memory. Future research could address these possibilities by using fMRI with awake infants to capture sensitive neural measures of episodic memory functions in the hippocampus, including pattern separation, relational binding, and pattern completion.

Outside of the hippocampus, we observed involvement of the mPFC in statistical learning. This is striking, given the dramatic changes in frontal lobe anatomy over development.<sup>43</sup> In adults, mPFC strongly interacts with the hippocampus during memory

formation, facilitating encoding based on related past experiences (i.e., schemas) to promote memory integration<sup>21</sup> and consolidation.<sup>44</sup> Indeed, mPFC has been linked to gradual statistical learning over days and weeks in rodents.<sup>22</sup> It remains to be seen whether this mechanism contributes to rapid statistical learning over minutes in human infants, as tested here. Evidence for frontal involvement in this task is broadly consistent with recent research suggesting that the frontal cortex plays an important role in infant cognition.<sup>45–47</sup> An important limitation of the current study is the inability of fMRI to distinguish whether evidence of statistical learning in the hippocampus originates in the hippocampus or is a reflection of processing in the mPFC, given their connectivity.

Another limitation of the current study is that we did not obtain a behavioral measure of statistical learning. Neural measures have proven sensitive to related forms of statistical learning that do not manifest strongly in behavior.<sup>23,26</sup> Indeed, fMRI activity can be viewed as a dependent measure to be added to the toolkit of infant cognition,<sup>11</sup> perhaps no less direct than traditional infant behavioral measures, such as looking time or skin conductance. We carefully designed our study so that the random blocks controlled for all aspects of structured blocks except the presence of regularities. Because these regularities do not exist in the stimulus per se but rather in the mind of the observer by linking experiences over time, we attribute observed neural differences to statistical learning. Nevertheless, it will be important for future studies to combine neural and behavioral measures, for example, by measuring predictive eye movements concurrently with fMRI activity and evaluating how they are related within and across participants.

To conclude, we present the first evidence that the hippocampus is recruited for learning in human infants. This demonstrates that brain systems used for learning throughout the lifespan can be available from some of the earliest stages of life. In turn, this provides a starting point for understanding how the human brain supports the prodigious amount of learning that occurs during infancy, establishing building blocks critical for subsequent growth and education.

#### STAR★METHODS

Detailed methods are provided in the online version of this paper and include the following:

- **KEY RESOURCES TABLE**
- **RESOURCE AVAILABILITY**
  - Lead contact
  - Materials availability
  - Data and code availability
- **EXPERIMENTAL MODEL AND SUBJECT DETAILS**
  - Participants
- **METHOD DETAILS**
  - Data acquisition
  - Procedure
  - Gaze coding
- **QUANTIFICATION AND STATISTICAL ANALYSIS**
  - Preprocessing
  - Regions of interest
  - Statistical analysis

### SUPPLEMENTAL INFORMATION

Supplemental information can be found online at <https://doi.org/10.1016/j.cub.2021.04.072>.

### ACKNOWLEDGMENTS

We thank all of the families who participated; K. Armstrong, C. Greenberg, J. Bu, L. Rait, and the entire Yale Baby School team for recruitment, scheduling, and administration; H. Faulkner, Y. Braverman, J. Fel, and J. Wu for help with gaze coding; B. Sherman for advice on hippocampal segmentation; and N. Wilson, R. Lee, L. Nystrom, N. DePinto, and R. Watts for technical support. We are grateful for internal funding from the Department of Psychology and Princeton Neuroscience Institute at Princeton University and from the Department of Psychology and Faculty of Arts and Sciences at Yale University. N.B.T.-B. was further supported by the Canadian Institute for Advanced Research and the James S. McDonnell Foundation (<https://doi.org/10.3717/2020-1208>).

### AUTHOR CONTRIBUTIONS

C.T.E., N.I.C., V.R.B., and N.B.T.-B. initially created the protocol. All authors collected the data. C.T.E., L.J.S., T.S.Y., and N.B.T.-B. developed the pipeline. C.T.E., L.J.S., and T.S.Y. performed the analyses. C.T.E. and N.B.T.-B. wrote the initial draft of the manuscript. All authors contributed to the editing of the manuscript.

### DECLARATION OF INTERESTS

The authors declare no competing interests.

### INCLUSION AND DIVERSITY

One or more of the authors of this paper self-identifies as an underrepresented ethnic minority in science. While citing references scientifically relevant for this work, we also actively worked to promote gender balance in our reference list. The author list of this paper includes contributors from the location where the research was conducted who participated in the data collection, design, analysis, and/or interpretation of the work.

Received: November 9, 2020

Revised: March 19, 2021

Accepted: April 28, 2021

Published: May 21, 2021

### REFERENCES

1. Corkin, S. (2013). *Permanent Present Tense: The Unforgettable Life of the Amnesic Patient, HM (Basic Books)*.

2. Akhtar, S., Justice, L.V., Morrison, C.M., and Conway, M.A. (2018). Fictional first memories. *Psychol. Sci.* 29, 1612–1619.
3. Keresztes, A., Ngo, C.T., Lindenberger, U., Werkle-Bergner, M., and Newcombe, N.S. (2018). Hippocampal maturation drives memory from generalization to specificity. *Trends Cogn. Sci.* 22, 676–686.
4. Richmond, J., and Nelson, C.A. (2009). Relational memory during infancy: evidence from eye tracking. *Dev. Sci.* 12, 549–556.
5. Gómez, R.L., and Edgin, J.O. (2016). The extended trajectory of hippocampal development: implications for early memory development and disorder. *Dev. Cogn. Neurosci.* 18, 57–69.
6. Nelson, C.A. (1995). The ontogeny of human memory: a cognitive neuroscience perspective. *Dev. Psychol.* 31, 723–738.
7. Schacter, D.L., and Moscovitch, M. (1984). Infants, amnesics, and dissociable memory systems. In *Infant Memory: Its Relation to Normal and Pathological Memory in Humans and Other Animals*, M. Moscovitch, ed. (Springer), pp. 173–216.
8. Arnold, S.E., and Trojanowski, J.Q. (1996). Human fetal hippocampal development: I. Cytoarchitecture, myeloarchitecture, and neuronal morphologic features. *J. Comp. Neurol.* 367, 274–292.
9. Uematsu, A., Matsui, M., Tanaka, C., Takahashi, T., Noguchi, K., Suzuki, M., and Nishijo, H. (2012). Developmental trajectories of amygdala and hippocampus from infancy to early adulthood in healthy individuals. *PLoS ONE* 7, e46970.
10. Ellis, C.T., and Turk-Browne, N.B. (2018). Infant fMRI: a model system for cognitive neuroscience. *Trends Cogn. Sci.* 22, 375–387.
11. Yates, T.S., Ellis, C.T., and Turk-Browne, N.B. (2021). The promise of awake behaving infant fMRI as a deep measure of cognition. *Curr. Opin. Behav. Sci.* 40, 5–11.
12. Ellis, C.T., Skalaban, L.J., Yates, T.S., Beijanki, V.R., Córdova, N.I., and Turk-Browne, N.B. (2020). Re-imagining fMRI for awake behaving infants. *Nat. Commun.* 11, 4523.
13. Fiser, J., and Aslin, R.N. (2002). Statistical learning of new visual feature combinations by infants. *Proc. Natl. Acad. Sci. USA* 99, 15822–15826.
14. Kirkham, N.Z., Slemmer, J.A., and Johnson, S.P. (2002). Visual statistical learning in infancy: evidence for a domain general learning mechanism. *Cognition* 83, B35–B42.
15. Saffran, J.R., Aslin, R.N., and Newport, E.L. (1996). Statistical learning by 8-month-old infants. *Science* 274, 1926–1928.
16. Schapiro, A.C., Turk-Browne, N.B., Botvinick, M.M., and Norman, K.A. (2017). Complementary learning systems within the hippocampus: a neural network modelling approach to reconciling episodic memory with statistical learning. *Philos. Trans. R. Soc. Lond. B Biol. Sci.* 372, 20160049.
17. Canada, K.L., Hancock, G.R., and Riggins, T. (2021). Modeling longitudinal changes in hippocampal subfields and relations with memory from early- to mid-childhood. *Dev. Cogn. Neurosci.* 48, 100947.
18. Malykhin, N.V., Lebel, R.M., Coupland, N.J., Wilman, A.H., and Carter, R. (2010). In vivo quantification of hippocampal subfields using 4.7 T fast spin echo imaging. *Neuroimage* 49, 1224–1230.
19. Hevner, R.F., and Kinney, H.C. (1996). Reciprocal entorhinal-hippocampal connections established by human fetal midgestation. *J. Comp. Neurol.* 372, 384–394.
20. Lavenex, P., and Banta Lavenex, P. (2013). Building hippocampal circuits to learn and remember: insights into the development of human memory. *Behav. Brain Res.* 254, 8–21.
21. Schlichting, M.L., Mumford, J.A., and Preston, A.R. (2015). Learning-related representational changes reveal dissociable integration and separation signatures in the hippocampus and prefrontal cortex. *Nat. Commun.* 6, 8151.
22. Richards, B.A., Xia, F., Santoro, A., Husse, J., Woodin, M.A., Josselyn, S.A., and Frankland, P.W. (2014). Patterns across multiple memories are identified over time. *Nat. Neurosci.* 17, 981–986.

23. Turk-Browne, N.B., Scholl, B.J., Chun, M.M., and Johnson, M.K. (2009). Neural evidence of statistical learning: efficient detection of visual regularities without awareness. *J. Cogn. Neurosci.* *21*, 1934–1945.
24. Morey, R.D., and Rouder, J.N. (2018). BayesFactor: computation of Bayes factors for common designs. <https://cran.r-project.org/web/packages/BayesFactor/index.html>.
25. Lee, M.D., and Wagenmakers, E.J. (2014). *Bayesian Cognitive Modeling: A Practical Course* (Cambridge University).
26. Schapiro, A.C., Kustner, L.V., and Turk-Browne, N.B. (2012). Shaping of object representations in the human medial temporal lobe based on temporal regularities. *Curr. Biol.* *22*, 1622–1627.
27. Raichle, M.E., MacLeod, A.M., Snyder, A.Z., Powers, W.J., Gusnard, D.A., and Shulman, G.L. (2001). A default mode of brain function. *Proc. Natl. Acad. Sci. USA* *98*, 676–682.
28. Biagi, L., Crespi, S.A., Tosetti, M., and Morrone, M.C. (2015). BOLD response selective to flow-motion in very young infants. *PLoS Biol.* *13*, e1002260.
29. Deen, B., Richardson, H., Dilks, D.D., Takahashi, A., Keil, B., Wald, L.L., Kanwisher, N., and Saxe, R. (2017). Organization of high-level visual cortex in human infants. *Nat. Commun.* *8*, 13995.
30. Dehaene-Lambertz, G., Dehaene, S., and Hertz-Pannier, L. (2002). Functional neuroimaging of speech perception in infants. *Science* *298*, 2013–2015.
31. Kumaran, D., and Maguire, E.A. (2006). An unexpected sequence of events: mismatch detection in the human hippocampus. *PLoS Biol.* *4*, e424.
32. Wolbers, T., and Büchel, C. (2005). Dissociable retrosplenial and hippocampal contributions to successful formation of survey representations. *J. Neurosci.* *25*, 3333–3340.
33. Kumaran, D., and Maguire, E.A. (2009). Novelty signals: a window into hippocampal information processing. *Trends Cogn. Sci.* *13*, 47–54.
34. Hindy, N.C., Ng, F.Y., and Turk-Browne, N.B. (2016). Linking pattern completion in the hippocampus to predictive coding in visual cortex. *Nat. Neurosci.* *19*, 665–667.
35. Sherman, B.E., and Turk-Browne, N.B. (2020). Statistical prediction of the future impairs episodic encoding of the present. *Proc. Natl. Acad. Sci. USA* *117*, 22760–22770.
36. Covington, N.V., Brown-Schmidt, S., and Duff, M.C. (2018). The necessity of the hippocampus for statistical learning. *J. Cogn. Neurosci.* *30*, 680–697.
37. Schapiro, A.C., Gregory, E., Landau, B., McCloskey, M., and Turk-Browne, N.B. (2014). The necessity of the medial temporal lobe for statistical learning. *J. Cogn. Neurosci.* *26*, 1736–1747.
38. McClelland, J.L., McNaughton, B.L., and O'Reilly, R.C. (1995). Why there are complementary learning systems in the hippocampus and neocortex: insights from the successes and failures of connectionist models of learning and memory. *Psychol. Rev.* *102*, 419–457.
39. DeMaster, D., Pathman, T., Lee, J.K., and Ghetti, S. (2014). Structural development of the hippocampus and episodic memory: developmental differences along the anterior/posterior axis. *Cereb. Cortex* *24*, 3036–3045.
40. Lee, J.K., Ekstrom, A.D., and Ghetti, S. (2014). Volume of hippocampal subfields and episodic memory in childhood and adolescence. *Neuroimage* *94*, 162–171.
41. Farooq, U., and Dragoi, G. (2019). Emergence of preconfigured and plastic time-compressed sequences in early postnatal development. *Science* *363*, 168–173.
42. Guskjolen, A., Kenney, J.W., de la Parra, J., Yeung, B.A., Josselyn, S.A., and Frankland, P.W. (2018). Recovery of “lost” infant memories in mice. *Curr. Biol.* *28*, 2283–2290.e3.
43. Matsuzawa, J., Matsui, M., Konishi, T., Noguchi, K., Gur, R.C., Bilker, W., and Miyawaki, T. (2001). Age-related volumetric changes of brain gray and white matter in healthy infants and children. *Cereb. Cortex* *11*, 335–342.
44. Tse, D., Takeuchi, T., Kakeyama, M., Kajii, Y., Okuno, H., Tohyama, C., Bito, H., and Morris, R.G.M. (2011). Schema-dependent gene activation and memory encoding in neocortex. *Science* *333*, 891–895.
45. Dehaene-Lambertz, G. (2017). The human infant brain: a neural architecture able to learn language. *Psychon. Bull. Rev.* *24*, 48–55.
46. Linke, A.C., Wild, C., Zubiaurre-Elorza, L., Herzmann, C., Duffy, H., Han, V.K., Lee, D.S.C., and Cusack, R. (2018). Disruption to functional networks in neonates with perinatal brain injury predicts motor skills at 8 months. *Neuroimage Clin.* *18*, 399–406.
47. Raz, G., and Saxe, R. (2020). Learning in infancy is active, endogenously motivated, and depends on the prefrontal cortices. *Annu. Rev. Dev. Psychol.* *2*, 247–268.
48. Fonov, V., Evans, A.C., Botteron, K., Almlí, C.R., McKinstry, R.C., and Collins, D.L.; Brain Development Cooperative Group (2011). Unbiased average age-appropriate atlases for pediatric studies. *Neuroimage* *54*, 313–327.
49. Aly, M., and Turk-Browne, N.B. (2016). Attention stabilizes representations in the human hippocampus. *Cereb. Cortex* *26*, 783–796.
50. Gousias, I.S., Hammers, A., Counsell, S.J., Srinivasan, L., Rutherford, M.A., Heckemann, R.A., Hajnal, J.V., Rueckert, D., and Edwards, A.D. (2013). Magnetic resonance imaging of the newborn brain: automatic segmentation of brain images into 50 anatomical regions. *PLoS ONE* *8*, e59990.
51. Dice, L.R. (1945). Measures of the amount of ecologic association between species. *Ecology* *26*, 297–302.
52. Yarkoni, T., Poldrack, R.A., Nichols, T.E., Van Essen, D.C., and Wager, T.D. (2011). Large-scale automated synthesis of human functional neuroimaging data. *Nat. Methods* *8*, 665–670.
53. Schlichting, M.L., Guarino, K.F., Schapiro, A.C., Turk-Browne, N.B., and Preston, A.R. (2017). Hippocampal structure predicts statistical learning and associative inference abilities during development. *J. Cogn. Neurosci.* *29*, 37–51.
54. Siegel, J.S., Power, J.D., Dubis, J.W., Vogel, A.C., Church, J.A., Schlaggar, B.L., and Petersen, S.E. (2014). Statistical improvements in functional magnetic resonance imaging analyses produced by censoring high-motion data points. *Hum. Brain Mapp.* *35*, 1981–1996.
55. Efron, B., and Tibshirani, R. (1986). Bootstrap methods for standard errors, confidence intervals, and other measures of statistical accuracy. *Stat. Sci.* *1*, 54–75.



## STAR★METHODS

### KEY RESOURCES TABLE

REAGENT or RESOURCE	SOURCE	IDENTIFIER
Deposited data		
Raw and preprocessed data	Dryad Digital Repository	<a href="https://doi.org/10.5061/dryad.2z34tmpmf">https://doi.org/10.5061/dryad.2z34tmpmf</a>
Software and algorithms		
MATLAB v. 2017a	Mathworks	<a href="https://www.mathworks.com">https://www.mathworks.com</a>
Python v. 3.6	Python Software Foundation	<a href="https://www.python.org">https://www.python.org</a>
FSL v. 5.0.9	FMRIB	<a href="https://fsl.fmrib.ox.ac.uk/fsl/fslwiki">https://fsl.fmrib.ox.ac.uk/fsl/fslwiki</a>
Experiment menu v. 1.1	Yale Turk-Browne Lab	<a href="https://github.com/ntblab/experiment_menu">https://github.com/ntblab/experiment_menu</a>
Infant neuropipe v. 1.3	Yale Turk-Browne Lab	<a href="https://github.com/ntblab/infant_neuropipe">https://github.com/ntblab/infant_neuropipe</a>

### RESOURCE AVAILABILITY

#### Lead contact

Further information and requests for resources should be directed to the Lead Contact, Nicholas Turk-Browne ([nicholas.turk-browne@yale.edu](mailto:nicholas.turk-browne@yale.edu)).

#### Materials availability

This study did not generate new materials.

#### Data and code availability

The code for running the statistical learning task can be found at: [https://github.com/ntblab/experiment\\_menu](https://github.com/ntblab/experiment_menu). The code for performing the analyses can be found at: [https://github.com/ntblab/infant\\_neuropipe/tree/StatLearning](https://github.com/ntblab/infant_neuropipe/tree/StatLearning). The data, including anonymized anatomical images, manually traced ROIs, and both raw and preprocessed functional images can be found at: <https://doi.org/10.5061/dryad.2z34tmpmf>.

### EXPERIMENTAL MODEL AND SUBJECT DETAILS

#### Participants

Data from 24 sessions with infants aged 3.6 to 23.1 months ( $M = 11.6$ ;  $SD = 5.8$ ; 14 female) met our minimum criteria for inclusion of six usable task blocks with at least one pair of Structured and Random blocks in each of the first and second halves of exposure ( $M = 11.8$  total blocks;  $M = 9.8$  usable blocks). This sample does not include data from 11 sessions with enough blocks only prior to exclusions for head motion, eye gaze, and counterbalancing ( $M = 9.8$  total blocks;  $M = 3.5$  usable blocks), or from 44 sessions without enough blocks even prior to exclusions ( $M = 3.6$  total blocks) where the infant instead participated in other experiments. This corresponds to 79 attempted scan sessions. In the final sample, 11 participants provided one session of usable data, five infants provided two sessions, and one infant provided three. These sessions occurred at least one month apart (range = 1.1–9.3) and so the data were treated separately, similar to prior work.<sup>29</sup> Of the 24 sessions, six were collected at the Scully Center for the Neuroscience of Mind and Behavior at Princeton University, four were collected at the Magnetic Resonance Research Center (MRRC) at Yale University, and 14 were collected at the Brain Imaging Center (BIC) at Yale University. Refer to [Table S1](#) for information on each session. Parents provided informed consent on behalf of their child. The study was approved by the Institutional Review Boards at Princeton University and Yale University.

### METHOD DETAILS

#### Data acquisition

Brain imaging data were acquired with a Siemens Skyra (3T) MRI at Princeton University and a Siemens Prisma (3T) MRI for both sites at Yale University, in all cases with the 20-channel Siemens head coil. Anatomical images were acquired with a T1-weighted PETRA sequence ( $TR_1 = 3.32$ ms,  $TR_2 = 2250$ ms,  $TE = 0.07$ ms, flip angle =  $6^\circ$ , matrix =  $320 \times 320$ , slices = 320, resolution = 0.94mm iso, radial slices = 30000). Functional images were acquired with a whole-brain T2\* gradient-echo EPI sequence that was the same at Princeton and Yale MRRC ( $TR = 2$  s;  $TE = 28$ ms; flip angle =  $71^\circ$ ; matrix =  $64 \times 64$ ; slices = 36; resolution = 3mm iso; interleaved slice acquisition) and almost identical at Yale BIC (except  $TE = 30$ ms; slices = 34).

## Procedure

Conducting fMRI research with awake infants presents many challenges. We have described and validated our protocol in detail in a separate methods paper.<sup>12</sup> In brief, families visited the lab prior to their first scanning session for an orientation session. This served to acclimate the infant and parent to the scanning environment. Scanning sessions were scheduled for a time when the parents felt the infant would be calm and happy. The infant and parent were extensively screened for metal. Hearing protection was applied to the infant in three layers: silicon inner ear putty, over-ear adhesive covers, and ear muffs. The infant was placed on the scanner bed, on top of a vacuum pillow that comfortably reduced movement. The top of the head coil was not used because the bottom elements provided sufficient coverage of the smaller infant head. We determined this in a previous study covering the same age range,<sup>12</sup> by measuring the signal strength in anterior and posterior portions of the brain. We found a similar proportion of signal drop-off in infants without the top of the head coil as we did in adults with the top of the head coil, owing to their smaller brains in closer proximity to the bottom elements. The lack of top coil created better visibility for monitoring infant comfort and allowed us to project stimuli onto the ceiling of the bore directly above the infant's face using a custom mirror system. A video camera (Princeton and Yale MRRC: MRC 12M-i camera; Yale BIC: MRC high-resolution camera) recorded the infant's face during scanning for monitoring and eye tracking. One or occasionally two parents remained in the scanner room within arm's reach of the infant at all times. They were accompanied by an experimenter who explained the process, answered questions, and directed the scan in collaboration with the parent(s). The experimenters were non-clinical staff experienced in developmental research. Either the parent or experimenter would comfort the child when necessary by, for example, holding their hand or patting their stomach.

When the infant was calm and focused, stimuli were shown in MATLAB using Psychtoolbox (<http://psychtoolbox.org>). The stimuli were colorful, fractal-like images used previously in studies of statistical learning in adults.<sup>26,34</sup> Images appeared every 1 s, looming in size from 2.4° of visual angle at onset to 14.6° at offset.<sup>14</sup> Each block contained 36 images presented sequentially one at a time in a unique order, followed by 6 s of rest with the screen blank.

Blocks alternated between Structured and Random conditions (Figure 2). Which condition appeared first was assigned randomly. Thus, the elapsed time from the start of the experiment was approximately matched between conditions. In the Structured condition, six fractals (A-F) were organized into three pairs (AB, CD, EF). The sequence of each block was generated by randomly inserting six repetitions of each pair. The first member of a pair (A, C, E) was always followed by the second (B, D, F, respectively) resulting in a transition probability of 1.0. After the second member of a pair, another pair began, resulting in a transition probability of 0.33 on average. In the Random condition, six different fractals (G-L) were presented individually. The sequence of each block was generated by randomly inserting six repetitions of each fractal, avoiding back-to-back repetitions of the same fractal. This resulted in a uniform transition probability of 0.20 on average. The six fractals in each condition were consistent across all blocks of that condition. For participants who attempted the experiment in more than one session, different stimuli were used across sessions.

## Gaze coding

Infant gaze was coded offline by two or more coders ( $M = 2.7$ ) blind to the block condition. The coders determined whether the gaze was on-screen, off-screen (i.e., blinking or looking away), or undetected (i.e., out of the camera's field of view or obscured by a hand or other object). Across coders, every video frame was coded at least once. The frame rate and resolution varied by camera and site, but the minimum rate was 16Hz and we always had sufficient resolution to identify the eye. The coded category for each frame was determined as the mode of a moving window of five frames centered on that frame across all coder reports. In case of a tie, the modal response from the previous frame was used. The coders were highly reliable: when coding the same frame, coders reported the same response on 93% (SD = 6%; range across sessions = 73%–99%) of frames. Infants included in the final sample looked at the stimulus 89% of the time on average (range = 80.3%–97.3%). Blocks were excluded if the eyes were off-screen for 50+% of the block. One participant did not have eye-tracking data due to a technical problem but real-time monitoring confirmed that their eyes were open and attending to the stimulus for at least 50% of each block.

## QUANTIFICATION AND STATISTICAL ANALYSIS

### Preprocessing

Individual runs were preprocessed using FEAT in FSL (<https://fsl.fmrib.ox.ac.uk/fsl/fslwiki/>), with modifications optimized for infant data. We discarded three volumes from the beginning of each run, in addition to the volumes automatically discarded by the EPI sequence. Blocks were stripped of any excess burn-in or burn-out volumes beyond the 3 TRs (6 s) of rest after each block. We attempted to collect all data within one run, lasting approximately 8.5 minutes. We did not finish the planned 12 blocks in 4 of the sessions because the parent or experimenter made a judgment call that the infant was not attentive to the display (e.g., falling asleep, distracted by camera or other objects in bore, lifting head). For 7 sessions, we took a break during data collection (break  $M = 637$  s; range = 115–1545 s). These breaks could involve switching to an anatomical scan or getting out of the scanner. If other tasks, not discussed here, were included in a run before or after this experiment, we excised them to form an experiment-specific pseudo-run ( $N = 12$  sessions).

The reference volume for alignment and motion correction was chosen as the 'centroid' volume with the minimal Euclidean distance from all other volumes. The slices in each volume were realigned with slice-time correction. Time-points were excluded if there was greater than 3 mm of movement from the previous time-point ( $M = 8.9\%$ ; range = 0.0%–21.3%). We interpolated rather than excised these time-points so that they did not bias the linear detrending (in later analyses these time-points were excised). Blocks

were excluded if 50+ % of the time-points were excluded. The mask of brain and non-brain voxels was created from the signal-to-fluctuating-noise ratio (SFNR) for each voxel in the centroid volume. The data were spatially smoothed with a Gaussian kernel (5 mm FWHM). Linear trends in time were removed using a high-pass filter to control for generic time-dependent effects unrelated to the task. The despiking algorithm in AFNI (<https://afni.nimh.nih.gov>) was used to attenuate aberrant time-points within voxels. This algorithm fits a curve to the voxel time series and finds the residuals of that curve. The variance in those residuals is computed and any time points that are outliers are removed via interpolation. For further explanation and justification of these preprocessing procedures, please see Ellis et al.<sup>12</sup>

We registered each run's centroid volume to the infant's anatomical scan from the same session. We used FLIRT with a normalized mutual information cost function for initial alignment. Supplemental manual registration was then performed using mrAlign from mrTools (Gardner lab) to fix deficiencies of automatic registration. The preprocessed functional data were aligned into anatomical space but kept in their original spatial resolution (3 mm iso). ROI analyses were performed within this native space of each participant. Whole-brain voxelwise analyses required further alignment of functional data into a standard space. The anatomical scan from each session was automatically (FLIRT) and manually (Freeview) aligned to an age-specific MNI infant template.<sup>48</sup> Combined with alignment of these templates to the adult MNI template (MNI152), the functional data were transformed into standard space. To determine which voxels to consider at the group level, the intersection of brain voxels from all infant participants in standard space was used as a whole-brain mask.

Because runs could contain different numbers of blocks from the Structured and Random conditions, blocks were only retained if they could be paired with a block from the other condition in the same run. This counterbalancing was enforced to ensure an equal amount of data in each condition. The blocks were labeled by the count of how many blocks from that condition had already been seen (henceforth, their 'seen-count'). For example, if an infant was watching the screen but moving too much in their first Structured block, then remained still in their second Structured block, the first usable block of that condition would be labeled with a seen-count of 2. Blocks were chosen to be paired across conditions so as to minimize the difference in seen-counts (i.e., to match the degree of exposure as best possible).

For an infant to be included, they needed to have at least three blocks from each condition, with at least one block in each condition from blocks 1 to 3 (first half) and at least one block in each condition from blocks 4 to 6 (second half). Using these criteria, the average number of included blocks for the usable sessions was 9.8 (SD = 1.9; range = 6–12), including 5.5 blocks in the first half and 4.3 blocks in the second half on average. There was no correlation between the number of included blocks and age ( $r = -0.05$ ;  $p = 0.788$ ). We did not find a difference between the proportion of Structured ( $M = 0.89$ ) and Random ( $M = 0.86$ ) blocks that were included ( $CI = [-0.019, 0.088]$ ;  $p = 0.210$ ). The block order was determined randomly, with 15 sessions starting with a Structured block and 9 sessions starting with a Random block (as reported in the main text, there were no reliable order effects on the neural results). To account for differences across runs in intensity and variance, the blocks that survived exclusions and balancing across conditions were normalized over time within run using z-scoring, prior to the runs being concatenated for further analyses.

### Regions of interest

The main analyses involved manually tracing ROIs in the medial temporal lobe (MTL) based on anatomical landmarks and then assessing evoked BOLD responses across voxels in these anatomical ROIs. To trace the ROIs, we extended a published protocol for MTL segmentation in adults<sup>49</sup> with help from protocols for hippocampal segmentation in infants.<sup>50</sup> The segmentation demarcated ROIs for the left and right hippocampus, each of which encompassed the subiculum, CA1, CA2/3, and dentate gyrus subfields. We did not segment these individual subfields because of the lack of validated anatomical guidelines for subfield boundaries in infants. For completeness, we also defined ROIs for the left and right MTL cortex (Figure S3), each of which contained entorhinal, perirhinal, and parahippocampal cortices (again not segmented individually).

To examine the reliability of the coder segmenting the infant hippocampus, we asked an expert in segmentation of the adult hippocampus to segment two of the infants. Using Dice similarity,<sup>51</sup> the consistency of labeling was 0.524 and 0.651 for the two participants across coders, indicating moderate reliability. Figure 1 shows example ROIs for two infants and the volume of each ROI across sessions as a function of age. The anterior hippocampus (volume:  $M = 1973.1 \text{ mm}^3$ ;  $SD = 537.5$ ) was defined as the head of the hippocampus, as manually traced,<sup>49</sup> and the posterior hippocampus (volume:  $M = 1796.4 \text{ mm}^3$ ;  $SD = 433.7$ ) was the remainder, including the body and tail. For one session (4.0 month old), the anatomical scan collected in the same session as the functional data was of insufficient quality for segmentation; we instead used the anatomical scan collected in their next session (at 6.0 months) and aligned the resulting segmentation to their functional data.

In a follow-up analysis, we defined ROIs for several nodes of the default mode network,<sup>27</sup> covering the posterior cingulate cortex, the right temporoparietal junction, the left temporoparietal junction, and the lateral temporal cortex (Figure S4). These ROIs were defined using the search term "default mode" in NeuroSynth<sup>52</sup> and clustering all contiguous voxels within these prominent regions. The ROIs were then tested akin to the hippocampus, as described below.

### Statistical analysis

For each infant, the volume of left and right hippocampus and MTL cortex ROIs was estimated by counting the number of voxels traced and multiplying by the volume of each voxel ( $0.82 \text{ mm}^3$ ). Whole-brain volume was calculated based on the number of voxels in the brain mask generated by applying Freesurfer (<https://surfer.nmr.mgh.harvard.edu>) to their anatomical scan.<sup>53</sup>

For the main analysis, a general linear model (GLM) was fit to the BOLD activity in each voxel using FEAT in FSL. The GLM contained four regressors: Structured and Random conditions in the first and second half of exposure. Each regressor modeled corresponding task blocks with a boxcar lasting the duration of stimulation convolved with a double-gamma hemodynamic response function. The assignment of blocks to halves was based on the seen-count: blocks with seen-count 1–3 were assigned to the first half and blocks with seen-count 4–6 were assigned to the second half. The six translation and rotation parameters from motion correction were included in the GLM as regressors of no interest. This controlled for movement-related changes in the BOLD response. Excluded TRs were scrubbed by including an additional regressor for each to-be-excluded time-point.<sup>54</sup> Contrasts of the resulting parameter estimates compared Structured greater than Random conditions separately for the first and second half; an interaction contrast compared the condition differences in the second versus first half. This controlled for generic time-effects, as the interaction corresponded to the increase for Structured blocks relative to interleaved Random blocks over exposure. The voxelwise z-statistic volumes for these contrasts were extracted for each session. ROI analyses averaged the z-statistics of all included voxels and examined the reliability of these averages at the group level. Whole-brain analyses examined the reliability of the z-statistics for each voxel across sessions.

Statistical analysis was performed on the ROI data using a non-parametric bootstrap resampling approach.<sup>55</sup> Namely, for each test we sampled 24 sessions with replacement 10,000 times, averaging across sessions on each iteration to generate a sampling distribution. For null hypothesis testing, we calculated the p value as the proportion of samples whose mean was in the opposite direction from the true effect, doubled to make the test two-tailed. To correct for multiple comparisons in whole-brain analyses, we used threshold-free cluster enhancement through the randomize function in FSL, resulting in voxel clusters  $p < 0.05$  corrected. A bootstrap resampling procedure was also used to statistically evaluate correlations, sampling bivariate data from 24 sessions with replacement 10,000 times, and calculating the Pearson correlation (or partial correlation) on each iteration. We calculated the p value as the proportion of samples resulting in a correlation with the opposite sign from the true correlation, doubled to make the test two-tailed. To investigate the interaction between anterior/posterior and left/right hippocampus, we compared the learning-related effect from each session in the GLM (Structured > Random in second versus first half) according to the interaction contrast: (Right anterior – Left anterior) – (Right posterior – Left posterior). We then applied bootstrap resampling on these values across sessions, as above, to determine significance.

We tested for differences in looking time during usable blocks using a similar approach. To test for a condition by half interaction, we compared the proportion of frames participants were coded as looking at the stimuli in each block type according to the contrast: (Structured second – Random second) – (Structured first – Random first). For the main effect of condition we used the contrast: (Structured second + Structured first) – (Random second + Random first). For the main effect of half we used the contrast: (Structured second + Random second) – (Structured first + Random first). For each test, we applied bootstrap resampling on the contrast values across sessions to determine significance.

To perform the time course analysis (Figure S2), we restricted analysis to pairs of Structured and Random blocks with identical seen-counts (as opposed to finding the closest match in the main analysis). This allowed us to separately examine the difference between Structured and Random at each of the 6 ordinal positions. This reduced the number of sessions with a sufficient number of usable blocks to 22, and the average number of usable blocks per retained session to 9.6 (SD = 1.9; range = 6–12). A GLM was fit to these data with a separate regressor for each block. The parameter estimates were labeled based on each block's seen-count and contrasted across conditions within the same seen-count. The resulting z-statistics were averaged across voxels within each ROI. The same bootstrap resampling approach with 1,000 iterations was used to assess statistical reliability and calculate p values for each ordinal position. An important feature of this approach is that we were able to estimate the time course even if individual subjects were missing one or more of the positions. This also takes into account the smaller sample size of sessions with later ordinal positions, because the obtained sampling distribution is more variable.